Microfabrication of Curved Sidewall Grooves Using Scanning Nanosecond Excimer Laser Ablation

Jing Gong*[a], Georgios Violakis[b] , Daniel Infante[b], Patrik Hoffmann[b], André Kostro[c], Andreas Schüler[a]

[a] Solar Energy and Building Physics Laboratory, EcolePolytechniqueFédérale de Lausanne (EPFL), CH-1015 Lausanne, Switzerland; [b] Laboratory for Advanced Materials Processing, Empa, Swiss Federal Laboratories for Materials Science and Technology, Feuerwerkerstrasse 39, CH-3602 Thun, Switzerland; [c] BASF Schweiz AG, Klybeckstrasse 141, CH-4057 Basel, Switzerland

ABSTRACT

Novel glazing with embedded micro-mirrors can significantly reduce the energy consumption due to cooling and lighting in buildings. Especially promising are large arrays of periodic micro compound-parabolic-concentrators (CPCs) with angular-selected transmittance. For the production of micro CPCs, curved sidewall grooves with a controlled optical surface and an aspect ratio of about 2.3 are fabricated on polycarbonate substrates by scanning nanosecond 248-nm excimer laser ablation. The likewise obtained microstructures can be used as master mold for replication. The cross-sections of the micro grooves are characterized by confocal microscopy, and the extracted morphologies are used for the ray-tracing simulation of the optical devices. Prior to the scanning ablation using a suitable mask in the optical path, the depth profiles under static ablation are investigated to identify ablation rate, imaging resolution and produced surface. Interestingly for the width of the mask opening being less than 6 μm, the ablation rate is increased due to optical interference and /or less shielding by debris. Concerning the scanning ablation, the depth of the curved sidewall grooves ranges from 48 μm to 114 μm, corresponding to the width of the groove opening being in the range from 20 μm to 50 μm. The observed final shapes in cross-sections are in good agreement with the design of the mask. For both theoretical and fabricated groove shapes, the angular-selected transmittance profiles predicted from ray-tracing simulations are highly similar. Scanning nanosecond excimer laser ablation is therefore a promising approach for the realization of high-quality micro CPCs.

Keywords: Advanced glazing, Micro compound parabolic concentrators, Curved sidewall grooves, Nanosecond excimer laser, Scanning ablation, Ray-tracing simulation

1. INTRODUCTION

Glazing of a building allows the penetration of natural light into buildings and builds the connection between occupants and exterior environment. The biological benefits of natural lightings and exterior view has been confirmed by researches[1,2]. However, glazing can cause severe overheating in summer due to its relatively high solar gain factor. Therefore, window design needs to fulfil its nature of providing daylight and external view while keeping a balanced energy performance of the building [3]. In order to solve the problems, a multifunctional glazing based on micro compound parabolic concentrators (CPCs) is proposed [4, 5]. The glazing consists of a polymer layer with a periodic array of embedded micro CPCs, and the polymer layer can be laminated to a glass pane of glazing. An important property of CPCs [6] is the acceptance angle. Light of the incoming angle within the acceptance range is concentrated and leaves the concentrator through the exit aperture of the structure, while the light out of acceptance angle will be reflected back to exterior through the input aperture. Thanks to the angular-selected transmittance of the CPCs, the proposed novel glazing can reduce energy consumption in cooling. Due to the light redirection by CPCs within the acceptance angle, the visual comfort inside a room can be improved. Moreover, because of the micrometric size of CPCs, a clear view seen through the glazing with embedded micro-mirrors is achieved, as indicated in Fig. 1 (a). The window system with micro-mirrors requires the fabrication of a master mold with well-defined microstructures of aspect ratio larger than 2 on a window-sized area. One or several steps of replications to transfer the microstructures from the

*Corresponding author email: jing.gong@epfl.ch, or hitgongjing@gmail.com
Tel.: +41- (0) 21 69 35557

Laser-based Micro- and Nanoprocessing XII, edited by Udo Klotzbach, Kunihiko Washio, Rainer Kling,
Proc. of SPIE Vol. 10520, 105200Z · © 2018 SPIE · CCC code: 0277-786X/18/$18 · doi: 10.1117/12.2286908

mold to a polymer film attached to a glass substrate are then needed. An example of the polymer microstructures attached on a glass substrate is shown in Fig. 1 (b). The dash lines show the surface where the highly reflective materials are deposited to form a CPC. After the deposition, the grooves of the microstructures are filled with the identical polymer and therefore embedded CPCs are achieved.

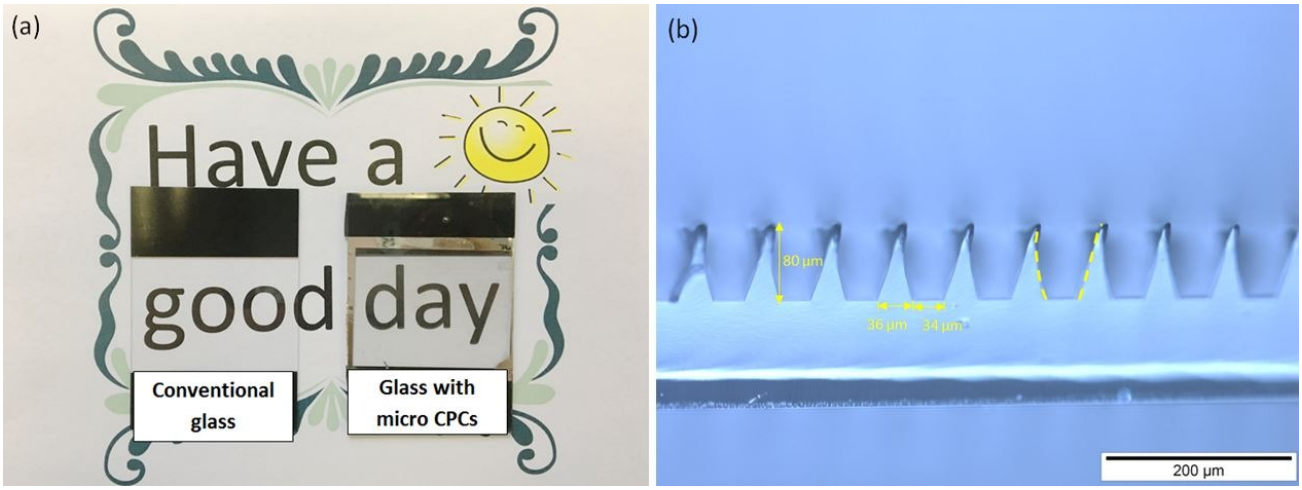

Fig. 1: (a) the views seen through the conventional glass and the glass with the polymer layer which consists of embedded micro CPCs. The viewing direction is perpendicular to the surface; (b) an example of polymer CPC microstructures transferred from the master mold to polymer microstructures on a glass substrate [5].

Concerning the master mold, fabrication of microstructures with aspect ratio larger than 2 and controlled curved sidewalls for window-sized area remains challenging. Electrical discharge machining makes use of electrical energy and turns it into thermal energy through a series of discrete electrical discharges occurring between the electrode and workpiece immersed in a dielectric fluid [7]. However, by nature EDM is made for cutting pieces but not for fabricating a large area microstructured surface for the use as windows. Lift-off is the process of exposing a pattern into photoresist, deposit a thin film over the entire area, and then washing away the photoresist to leave behind the film only in the patterned area. Therefore it is difficult to fabricate curve side walls with controlled optical surface [8]. Grey-scale direct laser writing uses masks with changing opacity makes it possible to fabricate curved side wall microstructures [9, 10]. However, the fabrication of gray-scale masks is complicated and costly. Moreover, the microstructured area is constrained by the size of the mask and precise stitching is required to have large area microstructured area.

In the present work, UV excimer laser ablation is used. Excimers are gas-type lasers of the ultraviolet (UV) or deep UV region with short pulse durations (normally 20 ns) [11]. The short wavelengths allow high-energy intensity and high resolution in machining. Compared with other types of lasers, excimer lasers can be more efficient for machining glass and polymer materials, where high precision and high surface quality machining is required. The machining mechanism for excimer lasers to remove material is usually mentioned as ablation, in which the irradiated material rapidly transforms into vapor due to localized thermal and partial direct bond breaking effect. The ejected species are in the form of atoms, molecules, ions, and clusters due to the interaction of an intense laser pulse with the material. Working at atmospheric pressure, the ejected species might partially redeposit on the substrate surrounding the ablation zones. Depending on the ablation conditions, the plume can interact with the light pulse, leading to deviation of the shapes of the final microstructures from the theoretical calculation. This article investigates the feasibility of the fabrication of the high-aspect ratio curved sidewall micro grooves at different scales. The shape fidelity from the mask to the final microstructures are studied. The optical properties of the final microstructures are also investigated by ray-tracing simulations.

2. EXPERIMENTS

A KrF excimer laser system (Lambda Physik LPX Pro) is used for the fabrication of the microstructures. The scanning mask projection method is applied in the present study. A 10 mm × 10 mm microlens array homogenized the laser beam

that illuminates a chrome on fused silica mask containing the structures to be transferred on the substrate. The mask is imaged by a 5 times reduction through a high-resolution projection objective onto the substrate at a typical fluence of 500 to 600 mJ/cm^2 [12]. A periodic array of elongated triangles with parabolic curved sidelines pattern is imaged and directly ablated in the substrate. During scanning laser ablation, the mask stage keeps stationary while the workpiece is moving at a constant speed. The desired 3D microstructures can be manufactured with appropriate mask design, precise motion of the stage and control of the laser operating parameters. The cross-section of the groove is determined by the shape of the mask as the ablation depth of the groove is inversely proportional to the ratio of the substrate step, s, between two consequent pulses, over the length of the structure L. The smaller the step, s, the deeper the structure will be, as the total dose on each spot of the substrate will be higher. The sketch of the configuration of the scanning excimer laser ablation and the resulting micro structure are shown schematically in Fig. 2. A ramp forms under the beam due to the scanning. The ramp angle ϑ between the ramp and the original substrate surface is decided by the total depth d_{tot} of the groove and the length of the irradiated spot L along the scanning direction, and the relation is expressed as:

$$\vartheta = \text{atan}(d_{tot}/L) \tag{1}$$

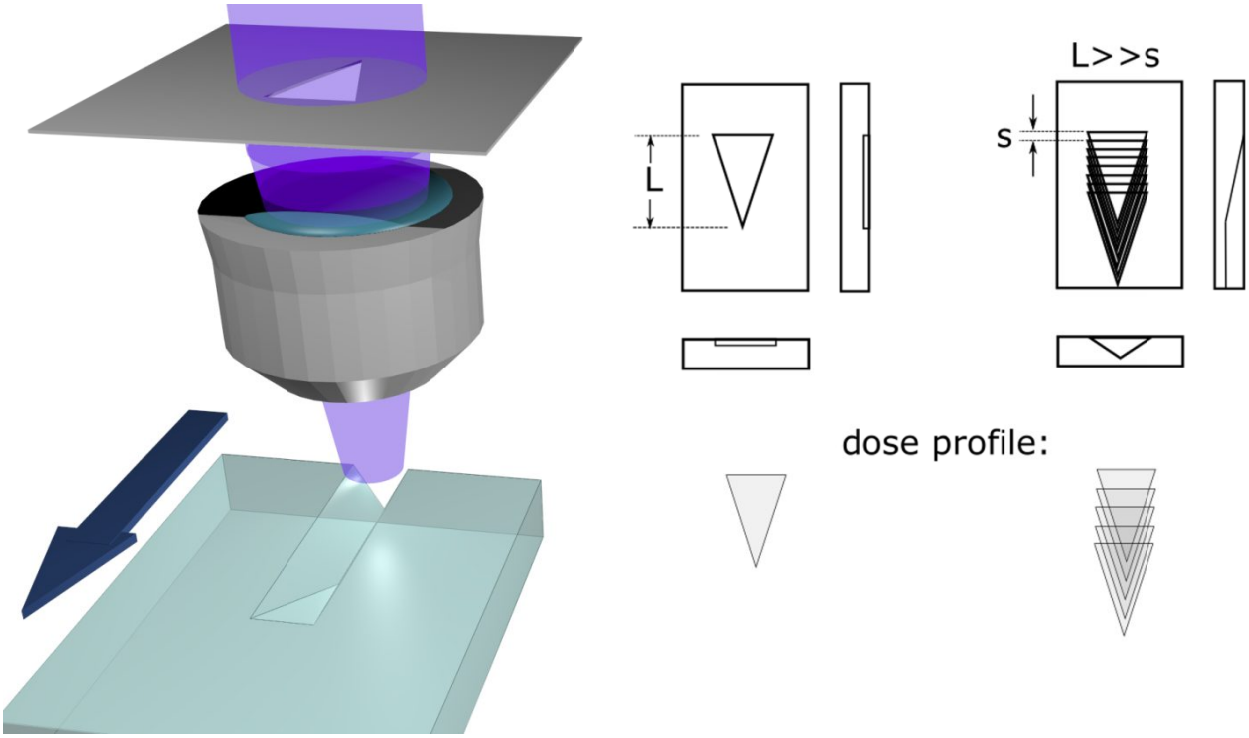

Fig. 2. Left: The sketch of the configuration of the scanning excimer laser ablation and the resulting micro structure. From top to bottom: Excimer laser beam, projection mask, objective lens, polycarbonate substrate. Right: Top, side and front view of a single and multiple shot exposure of the mask pattern on the substrate. As long as the motion step, s, of the substrate is shorter than that of the structure length, L, the total dose on the longer part will be higher resulting in deeper structures (more ablated material).

The application of the micro CPCs requires the fabrication of the high-aspect ratio curved sidewall micro grooves at different scales. The mask is designed based on the micro CPCs with the half acceptance angle of 30°. Three values of the opening of the groove are chosen: 22μm (marked as A), 37μm (B), and 50μm (C). The periodicity for structure A, B, C are 42 μm, 72 μm, and 100 μm. The aspect ratio for the three structures is about 2.3.

Concerning the operation parameters, the pulse repetition rate is set at 50 Hz. The duration of each pulse is fixed at 20 ns. The dragging speed for structure A, B, C are 72 μm/s, 57 μm/s and 49 μm/s to generate the desired depth. The speed is optimized by the numerical model to estimate the ablated depth *D*:

$$D = \frac{L}{V} \times f \times d_{static} \tag{2}$$

where V is the scanning speed, f corresponding to the repetition rate, and d_{static} is the ablation rate under static ablation for 20 pulses.

The specific values of the operating parameters can all be preset by a Computer-based controller. To guarantee high machining quality, the focus distance must be readjusted according to the sample thickness due to the limited depth of field of the laser projection system. The Polycarbonate (PC) sheet with 0.5 mm thickness made by Goodfellow is used as material for the scanning laser ablation because of its excellent ablation characteristics at the wavelength of 248 nm.

3. RESULTS AND DISCUSSION

3.1 Static ablation

The length of a unit opening on the mask for the three structures are 1300 μm, 1825 μm, and 2500 μm, respectively. The smallest openings on the mask are 10.5μm, 17 μm and 2.5 μm, respectively. Prior to the scanning ablation, static ablation are conducted to identify ablation rates, imaging resolution and produced surface. Lower rows of the Fig. 3 show the top surface microscope images of three different elongated triangular mask openings for CPCs on a PC substrate. The blowing gas direction is responsible for the weakly attached debris that is visible as asymmetric dark features above the triangles in Fig. 3. The bases of the triangles are about 22 μm, 37 μm, and 50 μm; with the lengths of the triangles of 260 μm, 365 μm, and 470μm, respectively. The contour graphs in the top row of Fig. 3, and the depth profiles along the lengths of the ablated triangles are presented after 20 pulses at 50 Hz static ablation. For the structure A and B, when the width of the projected triangular mask opening being less than 6 μm, deeper ablation is observed that can be explained either by optical interference effects and /or less plume shielding in tiny ablation regions or other unidentified reasons. The ablation rate for the region of the width larger than 6 μm is about 0.25 μm/pulse while for the region where the width is about 6 μm the ablation rate is almost twice, which is about 0.5 μm/pulse. This high ablation rate is kept until the visibly well-defined end of the triangle tip. This indicates that the mask opening at the end of the triangle is larger than the optical diffraction limit of the optical system that is about 2 μm. For the structure C, first the above mentioned effects result in an increased ablation depth of 0.5μm/pulse at a width of around 6 μm. Then with further decreasing width of the opening the ablation depth first increases to almost 0.5 μm/pulse and then decreases. The latter decrease of ablated depth is probably due to reaching the resolution limit of the projection system. Therefore the tip of the structure fades out and the resulted length is less than the theoretical calculation of using the length on the mask divided by the demagnification factor.

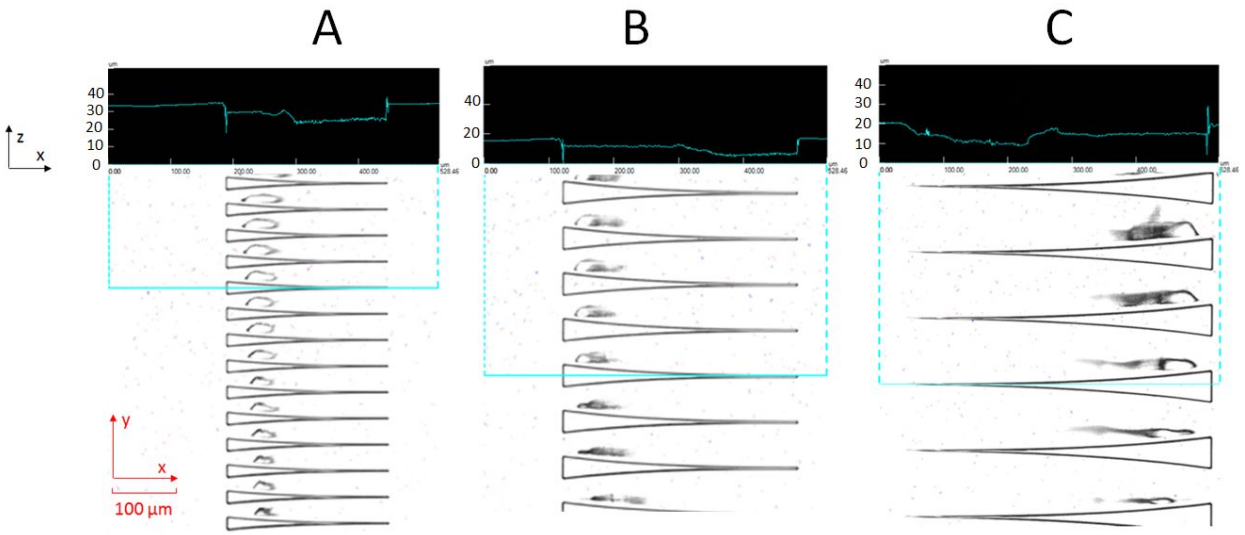

Fig. 3: The top-view microscope images of the three elongated triangular mask openings for the CPCs on a PC substrate.

3.2 Scanning ablation

Fig. 4 shows the cross-sections of the CPCs for A, B, and C on PC substrates. The curved shape of the sidewall is fabricated. The aspect ratio for the three structures is about 2.3. The depth for the micro grooves A, B, C are 48 μm, 84 μm, and 114 μm. Since the scanning speed for structure A, B, C are 72 μm/s, 57 μm/s and 49 μm, the calculated depth are 45 μm, 80 μm and 120 μm based on the formula (2). Therefore, the fabricated depth match well with the calculated depth. The average scanning ablation rate during fabrication are finally 0.15 μm/pulse, 0.14 μm/pulse, 0.11 μm/pulse in the center line of the grooves. With increasing depth, the loss of energy by heat conduction increases and thereby decreases the laser-induced temperature rise. Moreover, the transport of ablated species becomes less efficient and favors material re-condensation or deposition within the groove. For deep holes/grooves the attenuation of the incident light by scattering and secondary excitation of product species is important and becomes more efficient with increasing depth.

In order to further analyze the shape fidelity from the mask to a PC substrate, for each structure the profile of a unit groove is extracted from the microscope image of the cross-section, and it is compared with the theoretical profile, as shown in Fig. 5. The resulting curve sidewalls are not perfectly symmetric due to the blowing direction of the plume. Starting from 1/9 of the total ablated depth, the width of the fabricated groove tends to be larger than the theoretical design at the same depth. The relative average expansion of the width for structure A, B, C with respect to the maximum mask opening are approximately 4%, 2.4%, and 2.8%, respectively. Overall, the shape fidelity is considered to be good. Compared with structure A and B, it is observed that the curvature of the structure C is slightly better than those of structure A and B, possibly due to smaller ramp angle $\vartheta = \mathrm{atan}(d_{tot}/L)$, which leads to less direct debris on the sidewalls [13].

Scanning ablation by moving the substrate below the mask, as schematically presented in Fig. 2 appears to be a simple geometrical task in order to obtain wanted geometries of the side walls. However, there are several phenomena that increase the complexity of the estimation of the final shape of the ablation resulting topography. The ablation depth per pulse as most important parameter is actually influenced by several cross correlated parameters such as the already ablated depth, the ramp angle under which ablation takes place [14], the mask geometry (see for instance the depth profile of static ablated mask C in Fig. 3c), and potentially other parameters that we are not aware yet. In the present study no systematic modification of the mask geometry was performed in order to get the obtained results. Implementation of the above mentioned parameters into the scanning mask design is presently going on, and a mathematical model with the consideration of these parameters to predict the machined profiles will be established. The obtained structures are of surprising good quality, probably due to balancing counteraction of the above mentioned parameters. In order to explain the mechanism of achieving the correct shapes, the ablation of structure B is taken as example Going from the static ablation to the scanning ablation, the speed of sample displacement and the repetition rate of the laser together with the fixed fluence on the mask determine the depth of the groove after one full length of the triangle is scanned through. The ablation rate decreases with increasing depth of the structure. Observed from the top-view microscope images of the elongated triangular mask opening, 2/3 of ablation pulses come with half of the ablation rate, then about 1/3 of the ablation pulses result in the twice ablation rate per pulse. These two counteracting effects seem to result in the correct ablation of the shapes.

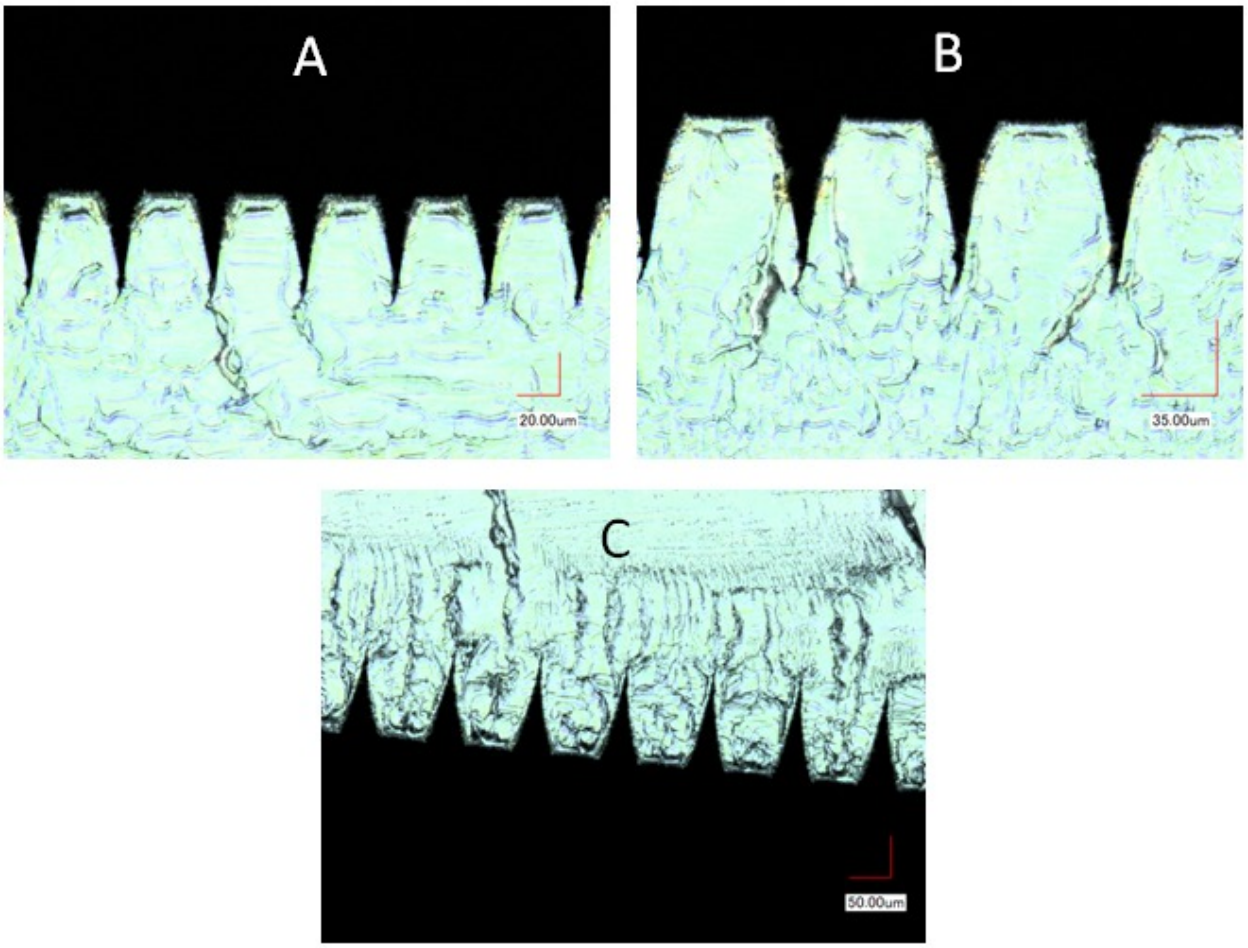

Fig. 4.: The cross-sections of the CPCs for A, B, and Con PC substrates.

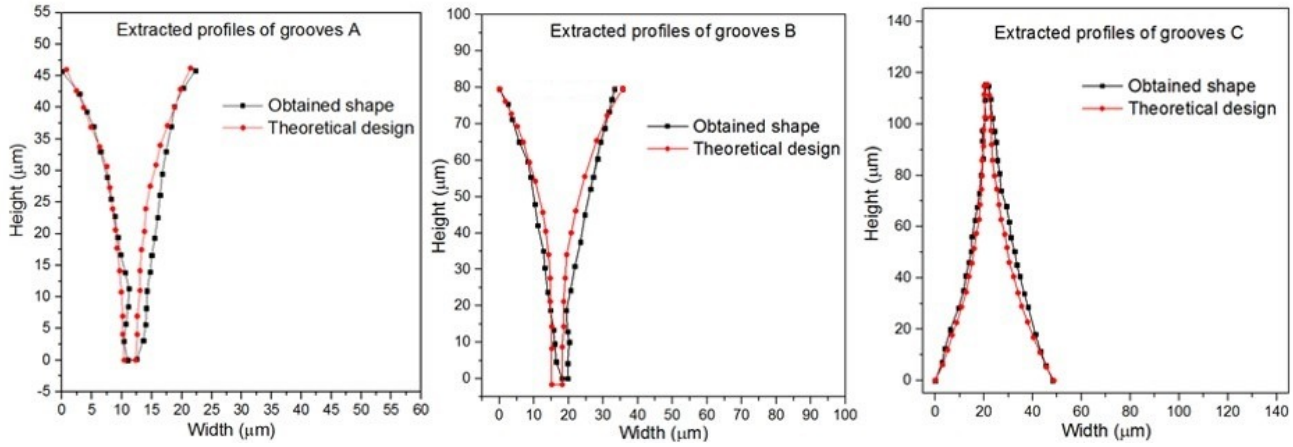

Fig. 5: The profiles of the fabricated grooves extracted from the microscope images and the theoretical design.

3.3 Simulation of the angular-dependent transmittance

The possible optical properties of the CPC based on structure B on a PC substrate is investigated using ray-tracing simulation [15]. The morphology of the cross-sections of both the blades and the polymer microstructures are extracted for building the computer model. In the computer model, the curve sidewalls are coated with highly reflective material (reflectance 0.9), as shown in Fig. 6. The theoretical design is of the half opening angle of 30°. The transmittance of the visible light as the function of elevation angles at the azimuth angle of 0˚ is calculated. The good agreement between the observed final shapes in cross-sections and the design of the mask, results in the highly similar angular-selective transmittance profiles predicted from ray-tracing simulations. The transmittance remains at about 0.95 in the angular range between -30˚ and 30˚, as the theoretical design is of half acceptance angle of 30°. Starting from 30˚, partial incident light is redirected by two or more times and then leave the system through the input aperture. Therefore, the transmittance significantly reduces beyond 30˚. The application of such angular feature can be used in the place where the winter is mild and summer is hot, or the elevation angle of the winter sun for the working hours are lower than 30˚

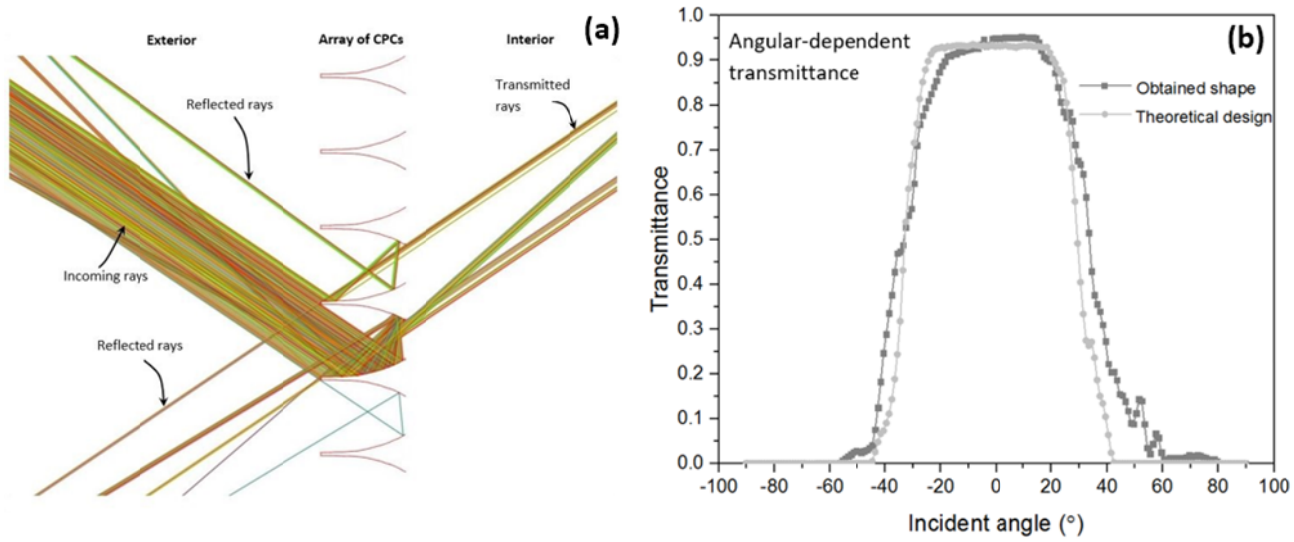

Fig. 6: (a) Computer model with extracted profile of the theoretical design for ray-tracing simulation; (b) calculated angular-dependent transmittance at the azimuth angle of 0°.

4. CONCLUSIONS

Large arrays of micro compound-parabolic-concentrators (CPCs) with angular-selected transmittance are promising to reduce energy consumption in buildings. For the production of micro CPCs, curved sidewall grooves with a controlled optical surface and an aspect ratio of about 2.3 are fabricated on polycarbonate substrates by scanning nanosecond 248-nm excimer laser ablation. The shapes of the obtained grooves are in good agreement with the design of the mask. For both theoretical and fabricated groove shapes, the angular-selected transmittance profiles predicted from ray-tracing simulations are highly similar. Scanning nanosecond excimer laser ablation is therefore a promising approach for the realization of high-quality micro CPCs.

5. ACKNOWLEDGEMENTS

This research has been financially supported by the Energy Funding Program of CTI within the Swiss Competence Center for Energy Research (SCCER) for Future Energy Efficient Buildings & Districts (FEEB&D).

6. REFERENCES

[1] Demir, A., & Konan, A. P. D. N. (2013). Impact of daylighting on student and teacher performance. Journal of Educational and Instructional Studies in the World, 3(1), 7.

[2] Chang, C. Y., & Chen, P. K. (2005). Human response to window views and indoor plants in the workplace. HortScience, 40(5), 1354-1359.

[3] Bodart, M., & De Herde, A. (2002). Global energy savings in offices buildings by the use of daylighting. Energy and Buildings, 34(5), 421-429.

[4] Gong, J., Kostro, A., Motamed, A., & Schueler, A. (2016). Potential advantages of a multifunctional complex fenestration system with embedded micro-mirrors in daylighting. Solar Energy, 139, 412-425.

[5] Gong, J., Kostro, A. & Schueler, A. (2018). TOWARDS NOVEL GLAZING WITH SEASONAL DYNAMICS BASED ON MICRO COMPOUND PARABOLIC CONCENTRATORS, Solar World Congress 2017, Abu Dhabi, United Arab Emirates, to be published.

[6] Rabl, A. (1976). Comparison of solar concentrators. Solar Energy, 18(2), 93-111.

[7] Ho, K. H., & Newman, S. T. (2003). State of the art electrical discharge machining (EDM). International Journal of Machine Tools and Manufacture, 43(13), 1287-1300.

[8] Bratton, D., Yang, D., Dai, J., & Ober, C. K. (2006). Recent progress in high resolution lithography. Polymers for Advanced Technologies, 17(2), 94-103.

[9]Yao, J., Cui, Z., Gao, F., Zhang, Y., Guo, Y., Du, C., ... &Qiu, C. (2001). Refractive micro lens array made of dichromate gelatin with gray-tone photolithography. Microelectronic Engineering, 57, 729-735.

[10] David, C., Wei, J., Lippert, T., &Wokaun, A. (2001). Diffractive grey-tone phase masks for laser ablation lithography. Microelectronic Engineering, 57, 453-460.

[11] Hocheng, H., & Wang, K. Y. (2008). Microgroove pattern machined by excimer laser dragging. International Journal of Manufacturing Technology and Management, 13(2-4), 241-253.

[12] Rowthu, S., Böhlen, K., Bowen, P., & Hoffmann, P. (2015). Surface 3D Micro Free Forms: Multifunctional Microstructured Mesoporous α-Alumina by in Situ Slip Casting Using Excimer Laser Ablated Polycarbonate Molds. ACS applied materials & interfaces, 7(44), 24458-24469.

[13] Wagner, F., & Hoffmann, P. (1999). Structure formation in excimer laser ablation of stretched poly (ethylene therephthalate)(PET): the influence of scanning ablation. Applied Physics A: Materials Science & Processing, 69(7), S841-S844.

[14] Pedder, J. E., & Holmes, A. S. (2006, February). A study of angular dependence in the ablation rate of polymers by nanosecond pulses. In Proc. of SPIE Vol (Vol. 6106, pp. 61061B-1).

[15] Kostro, A., Geiger, M., Scartezzini, J. L., &Schüler, A. (2016). CFSpro: ray tracing for design and optimization of complex fenestration systems using mixed dimensionality approach. Applied optics, 55(19), 5127-5134.